THE USE OF A HIGH LIMESTONE CONTENT MINING WASTE AS A SORBENT FOR CO_2 CAPTURE

R. C. Barbosa, J. J. R. Damasceno and C. E. Hori[*]

Faculdade de Engenharia Química, Universidade Federal de Uberlandia.
Av. João Naves de Ávila 2121, Bloco 1K, Campus Santa Mônica,
CEP: 38408-144, Uberlandia - MG, Brazil.
Fax: (55) (34) 3239-4249
E-mail: cehori@ufu.br

Abstract - In this work, a high limestone content waste was evaluated as a potential material for CO_2 capture. The influence of calcination conditions on the CO_2 capture capacity was evaluated using 5 cycles of calcination-hydration-carbonation reactions. A Central Composite Design of Experiments was set using calcination temperatures and time as variables. The response evaluated was the CO_2 capture measured by thermogravimetric analysis. The results indicate that both calcination temperature and time influence the CO_2 capture capacities in the initial cycles but, after a large number of cycles, the effect becomes less relevant. The optimum calcination temperature did not change significantly between cycles - about 893 °C in the first and 850 °C in the fourth cycle. However, the optimum calcination time decreased from 40.1 min in the first to 22.5 min in the fourth cycle. The maximum CO_2 capture capacity declines over the reaction cycles due to the sorbent sintering, which becomes more noticeable. Moreover, the waste used in this work is suitable for separating CO_2 from flue gas, achieving more than 0.2 g/g of capture capacity after five cycles.
Keywords: CO_2 capture; Limestone; Calcium oxide; Calcium carbonate.

INTRODUCTION

The continuous increase of atmospheric carbon dioxide levels since the Industrial Revolution, mostly due to fossil fuel combustion (Yu *et al*., 2012), has encouraged extensive research to develop technologies to reduce this gas emission (Phalak *et al*., 2012). CO_2 capture technologies are being implemented and could become a necessary option to achieve the necessary reduction (Zeman, 2007). This process consists of three steps: separation of CO_2 from flue gas – the most expensive step-, transport and sequestration.

Among the promising technologies to separate CO_2 by post-combustion capture processes, carbonation-calcination loops use an extremely cheap and abundant regenerable sorbent (Abanades *et al*., 2004; López-Periago *et al*., 2013): calcium carbonate. This process is based on the cycles of the gas–solid reaction (carbonation) of calcium oxide with carbon dioxide, forming calcium carbonate ($CaCO_3$) (Barker, 1973; Santos *et al*., 2012) and the reverse reaction (calcination) to regenerate the CaO, releasing a concentrated stream of CO_2 (Phalak *et al*., 2012) which can be stored or used for other purposes such as dry ice, refrigeration equipment, carbonated beverages and fire extinguishing equipment (Kikkinides and Yang, 1993).

Despite low costs, CaO-based sorbents show a fast deactivation and a decrease in their CO_2 capture capacity over reaction cycles because of sintering phenomena, crystal growth and pore blocking during the

calcination step (Abanades and Alvarez, 2003; Symonds *et al.*, 2009; Grasa and Abanades, 2006; González *et al.*, 2008; Manovic *et al.*, 2009; Kuramoto, 2003). Previous studies show that high calcination temperatures accelerate this deactivation process (Grasa and Abanades, 2006; González *et al.*, 2008). In order to overcome the sintering and enhance the sorbent reactivity, a range of methods has been proposed, such as doping of CaO-based sorbents (Al-Jeboori *et al.*, 2012) to produce synthetic sorbents, thermal preactivation of fresh sorbent (Valverde *et al.*, 2013) and hydrating (Yu *et al.*, 2012; Phalak *et al.*, 2012; Blamey *et al.*, 2010). A number of authors have shown that including an intermediate hydration of CaO improves the sorbent morphology, forming porous agglomerates (Kuramoto, 2003) and enhancing pore size, likely a shift from smaller to larger pores, which avoids the pore pluggage (Yu *et al.*, 2012; Phalak *et al.*, 2012).

Previous studies investigating carbonation of $Ca(OH)_2$ and carbonation of CaO show that $Ca(OH)_2$ reaches a higher conversion than CaO (Nikulshina *et al.*, 2007; Kuramoto *et al.*, 2003), whereas the carbonation of CaO is initially chemically controlled and then becomes controlled by diffusion, while the carbonation of $Ca(OH)_2$ at high temperatures (up to 400 °C) is all chemically controlled (Nikulshina *et al.*, 2007).

Usually the studies that use calcium carbonate as a potential sorbent for CO_2 capture processes are conducted with freshly mined materials. Although this type of material is cheap and abundant, the environmental impact of a mining process is always high. Therefore, it would be more environmentally friendly to use a residue as a CO_2 sorbent. Consequently, this work concerns the evaluation of a high limestone content waste from Vale Fertilizantes produced in an apatite concentration process for separating CO_2 through calcination-hydration-carbonation reactions under different calcination conditions to determine the optimum calcination temperature and time to provide the best performance.
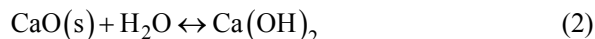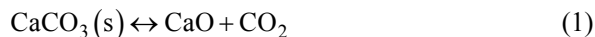
EXPERIMENTAL

Reaction Cycles

A set of 5 cycles (calcination−hydration−carbonation) was performed for each calcination condition, keeping the hydration and carbonation conditions constant. These conditions were fixed because there are studies in the literature which pointed out that the calcination step is usually the most critical one in

terms of sintering the sorbent materials (Ramkumar *et al.*, 2010).

The reactions developed in this work are provided below:

$$CaCO_3(s) \leftrightarrow CaO + CO_2 \tag{1}$$

$$CaO(s) + H_2O \leftrightarrow Ca(OH)_2 \tag{2}$$

$$Ca(OH)_2(s) + CO_2 \leftrightarrow CaCO_3 + H_2O \tag{3}$$

The samples were calcined in a muffle furnace under 30 mL/min of synthetic air flow. Calcination temperatures and time ranges of 723-977 °C and 11-49 min, respectively, were set by central composite design of the experiments, with five replicates in the central point (850 °C and 30 min) and an alpha orthogonality factor of 1.267. Table 1 shows an experimental matrix set by the central composite design. Thereby, for each cycle, 13 runs were performed, for different calcination temperatures and times.

**Table 1: Conditions of the Central Composite Design.**

Variable	-α	-1	0	1	+α
Calcination Temperature (°C)	723	750	850	950	977
Calcination Time (min)	11	15	30	45	49

The hydration and carbonation reactions were carried out under fixed conditions in a laboratory-scale fixed-bed reactor with internal diameter of 0.012 m and length of 0.317 m. The solid samples, after each calcination, were supported in this reactor using quartz wool, forming a packed bed and the reactor was placed in a heated zone provided by an electrical tube furnace. Liquid water was pumped at 25 °C, heated to 150 °C and then fed to the reactor as steam. Hydration was carried out at 500 °C for 30 min (Phalak *et al.*, 2012) under 90% steam and 10% argon. Carbonation was performed at 650 °C and 30 min (Phalak *et al.*, 2012) under 10% CO_2 (balanced with an argon stream).

Figure 1 shows schematically the experimental setup used to perform the cycle of reactions.

Characterization

The crystalline phases of the waste and the extent of calcination and carbonation were tested using X-ray diffraction analysis, on a Rigaku Miniflex diffractometer with CuKα radiation at 30 kV and 30 mA. The analyses were performed varying 2θ from 5 to 90 °, with steps of 0.02 ° and a time of 2 seconds per step.
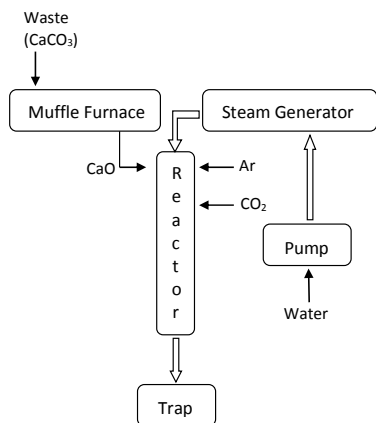
Figure 1: Schematic drawing of the experimental system used for the calcination-hydration-carbonation reaction cycles.

Average crystallite size after first and fifth calcinations was estimated with the Scherrer equation:

$$D = \frac{\kappa\lambda}{\beta\cos\theta} \tag{4}$$

where D is the mean size of the crystallite; κ is the Scherrer constant, which depends on the shape factor, with a typical value of about 0.9; λ is the X-ray wavelength; $\beta(2\theta)$ is the line broadening at half the maximum intensity, in radians; and θ is the Bragg angle.

The BET surface area was determined from N_2 adsorption isotherms, at 77 K, using a Quantachrome adsorption analyser model Quantsorb Jr.

CO₂ Capture Capacity

A thermogravimetric analysis (TGA) was used to evaluate the extent of CO_2 capture in the cycles. After each carbonation step, about 5 mg of sample was tested in the TGA. The analyses were carried out under N_2 flow and the same conditions used in the calcination step. Thus, if the sample was calcined at 750 °C for 15 min, in the TGA test the sample was heated from 25 to 750 °C under N_2 and held isothermally at 750 °C for 15 min.

Reactivity of Calcium Oxide

The reactivity of the oxide formed was experimentally studied following the procedure described by ASTM - C - 110-76. This methodology is based on the temperature increase due to the heat released during the hydration reaction of the oxide. After each calcination, around 2.5 g of sample and 10 g of water were introduced into an adiabatic receiver and shaken by a magnetic stirrer. The increase of the temperature

was monitored using a thermometer placed inside the receiver and the temperature variation reached after 10 min was recorded.

RESULTS

A diffractogram of the waste is shown in Figure 2. As can be seen, the waste is composed mostly of calcium carbonate. Calcite ($CaCO_3$, rhombohedral) is the predominant phase. Limestone with a high concentration of calcite has received the most focus for CO_2 capture because it allows the highest capture of CO_2 per unit mass (Blamey *et al*. 2010). The waste has a specific surface area of 3 m^2/g, as determined by BET.
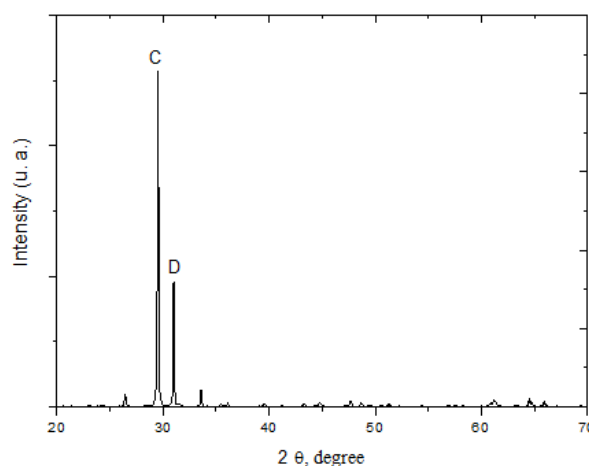

Figure 2: XRD diffraction pattern of waste as received. C – Calcite (JCPDS 01-072-1651) and D – Dolomite (JCPDS 01-071-1662).

Figure 3 shows XRD diffraction patterns of samples after the first and the second carbonation cycles and Figure 4 after the first and the second calcination. Both samples were calcined at 950 °C for 45 min and carbonated at 650 °C for 30 min. It can be seen that the carbonations and calcinations are reversible in practice since, after the first and second carbonations, there is only calcium carbonate and after calcinations there is mostly calcium oxide. Kuramoto *et al*. (2003) also reported that the sorbent regenerates, maintaining the CO_2 capture capacities of this type of mineral over calcination-hydration-carbonation cycles. The authors compared the results with and without intermediate hydration of CaO, suggesting that the hydration treatment provides the durability of the sorbents in repetitive CO_2 sorption.

Figure 4 shows the diffractograms of a sample after the first and fifth calcination cycles. The increase of intensity of the major peaks is evidence that the

sample is sintering as it is submitted to calcination-hydration–carbonation cycles. After the first and fifth calcination the average crystallite sizes for the $CaCO_3$ phase obtained using the Scherrer equation were (0.298 mm) and (0.340 mm) respectively. This shows that $CaCO_3$ particles are sintering during the cycles, which makes their diameter larger and decreases their surface area. Besides the $CaCO_3$ phase, one can also notice some small peaks of MgO due to calcined dolomite and some peaks of $Ca(OH)_2$, probably due to the contact of the oxide with air moisture.
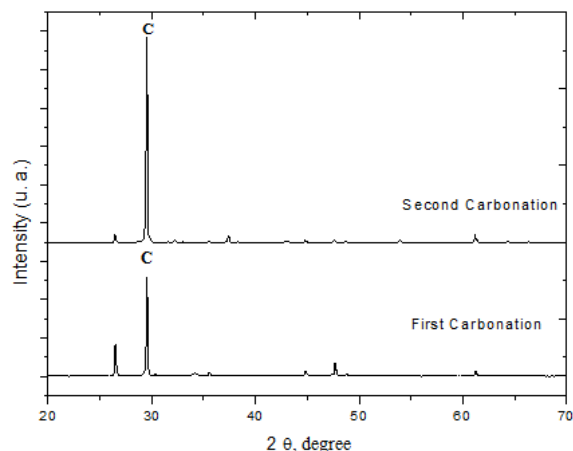
Figure 3: Diffractograms of the carbonation product after the first and second cycles. C – Calcite (JCPDS 01-072-1651). Calcination carried out at 950 °C for 45 min, hydration at 500 °C for 30 min and carbonation at 650 °C for 30 min.
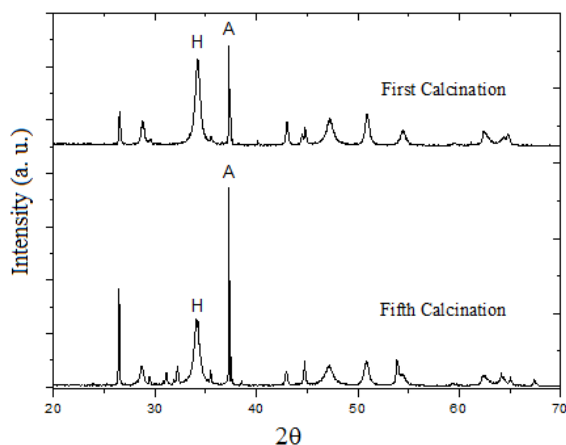

Figure 4: Diffractograms of the calcination product after the first and fifth cycles. A - CaO (JCPDS 01-082-1690) and H - $Ca(OH)_2$ (JCPDS 04-0733). Calcination carried out at 950 °C for 45 min, hydration at 500 °C for 30 min and carbonation at 650 °C for 30 min.

The extent of CO_2 captured during the cycles, for different calcination conditions, is shown in Figure 5.

As can be seen, samples calcined at temperatures up to 800 °C performed better in the first cycle. It can be noted that the CO_2 capture capacity drops from the second to fifth cycle for all samples. However, as the number of cycles increases, the CO_2 capture capacity seems to stabilize. Similar results were obtained by Rhida *et al*. (2012) working with natural limestones and pellets prepared from acetified limestone, with kaolin binder or with $Al(OH)_3$ binder. Therefore, the calcination temperature seems to have a pronounced effect on CO_2 capture in the first cycle, since samples calcined at higher temperatures performed much better. However the effect diminishes with increasing number of cycles, and all samples achieved similar CO_2 uptake in the fifth cycle.

In Figure 5 it can be seen that samples calcined at temperatures up to 800 °C achieved almost 0.4 g/g of CO_2 capture capacity in the first cycle and about 0.22 g/g in the fifth cycle. In a study using natural limestones, Rhida *et al*. (2012) obtained about 0.5 g/g to 0.24 g/g, in the first and fifth cycle, respectively. This result suggests that the waste used in this work is suitable for separating CO_2 from flue gas.
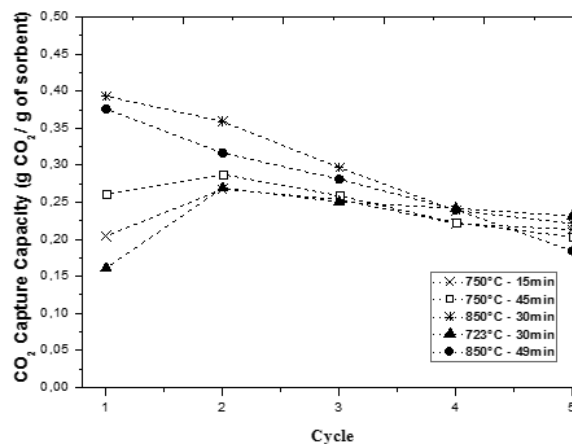
Figure 5: CO_2 Capture Capacity vs. the number of cycles under different calcination conditions.

Another interesting effect can be noted in Figure 5: the samples calcined at lower temperatures showed an increase in the CO_2 uptake from the first to second cycle. This probably happened because the use of lower temperatures is not sufficient to decompose completely $CaCO_3$ into CaO in the first cycle. Figure 6 shows XRD data for a sample calcined at 800 ºC for 5 minutes (Fig. 6A) and for 30 minutes (Fig. 6B). The presence of a small $CaCO_3$ diffraction peak (2θ around 30º) in Fig. 6B indicates that the use of a temperature of 800 ºC is not sufficient to calcine completely the sample, even after 30 minutes. Therefore,

the use of temperatures below 800 ºC, such as 723 ºC and 750 ºC (shown in Figure 5) are possibly insufficient to convert all the $CaCO_3$ into CaO, even if longer calcination times are used. After the second calcination–hydration–carbonation cycle, probably all $CaCO_3$ was converted to CaO.

Figure 7 shows the response surface for each cycle. In the first and second cycles, the CO_2 capture capacity increased, as the calcination temperature increased, until reached the best region and then began to decline. This is expected because, for low calcination temperature and time, there is probably still unreacted carbonate in the first cycles and, as the calcination temperature and time increase, the sorbent become less reactive due to the sintering processes. However, from the third to fifth cycles the ability to capture CO_2 for all conditions tends to the same value. For a larger number of cycles, it seems reasonable to assume that the decay in CO_2 capture capacity would be more dependent on the amount of cycles than on the calcination conditions, within this experimental range.

The maximum capacity declined over the cycles. For instance, in the first cycle, the maximum CO_2 capture capacity was around 0.42 gram of CO_2 per gram of waste and in the fifth cycle, it was only about 0.23. Previous studies investigating CO_2 capture with the same type of materials also show the decay in the maximum capture capacity along the cycles (Grasa and Abanades, 2006; González et al., 2008). Usually this decline in the CO_2 capture capacities is attributed to the sintering phenomena (Abanades and Alvarez, 2003; Symonds et al., 2009) which becomes more noticeable with each cycle and is enhanced by increasing calcination temperatures (Borgwardt, 1989).

The optimum conditions for each reaction cycle are shown in Table 2. For the fifth cycle, the optimum conditions were out of the experimental region.

Table 2: Optimum conditions for CO₂ capture capacity.

Cycle	X_1	X_2	Calcination Temperature (°C)	Calcination time (min)
1°	0.43	0.67	893	40.1
2°	0.33	0.17	883	32.6
3°	0.25	0.50	875	37.5
4°	0	-0.50	850	22.5

The CO_2 capture capacities for the first to fifth cycles can be described by Equations (5) to (9), respectively.
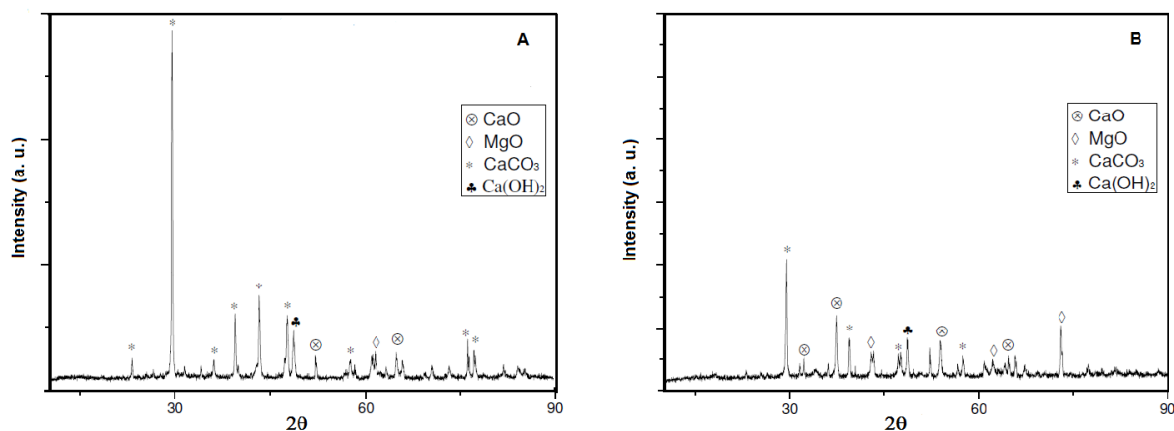
$$Y = 0.39 + 0.06 * X_1 + 0.04 * X_2$$
$$-0.07 * X_1^2 - 0.03 * X_2^2 \tag{5}$$

$$Y = 0.35 + 0.02 * X_1 + 0.01 X_2$$
$$-0.03 * X_1^2 - 0.03 * X_2^2 \tag{6}$$

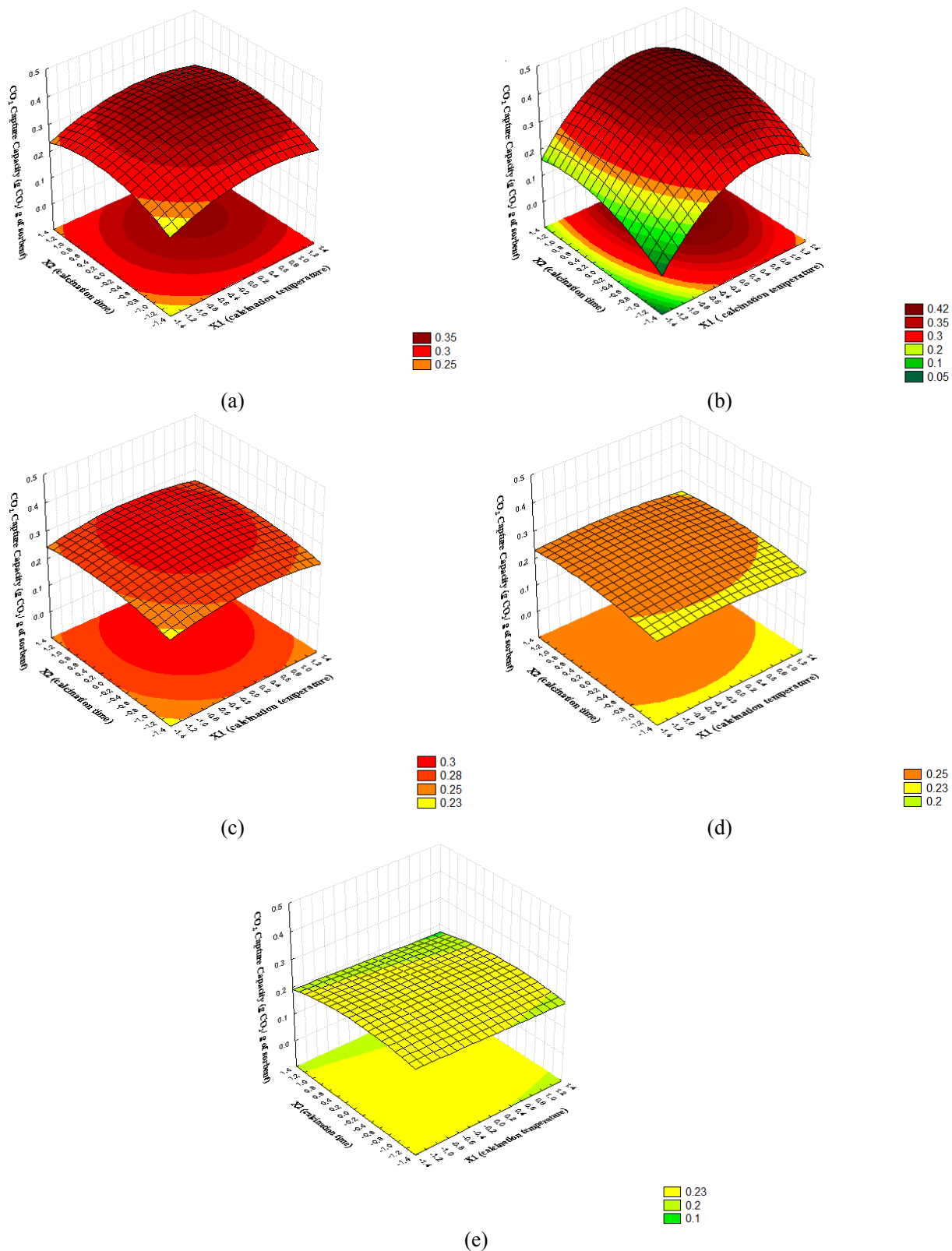$$Y = 0.29 + 0.01 * X_1 + 0.01 * X_2$$
$$-0.02 * X_1^2 - 0.01 * X_2^2 \tag{7}$$

$$Y = 0.25 - 0.01 * X_2 - 0.01 * X_1^2 - 0.01 * X_2^2 \tag{8}$$

$$Y = 0.22 - 0.01 * X_1 - 0.01 * X_2 - 0.01 * X_2^2 \tag{9}$$

Figure 6: Diffractograms of samples calcined at 800 ºC. A – for 5 minutes; B – for 30 minutes. (CaO - JCPDS 01-082-1690; CaCO₃ - JCPDS 01-072-1651; MgO - JCPDS 01-079-0612; Ca(OH)₂ - JCPDS 04-0733).

(a)   (b)

(c)   (d)

(e)

Figure 7: Response Surface of the Capture Capacity. (a) First Cycle; (b) second cycle; (c) third cycle; (d) fourth cycle, (e) fifth cycle.

Results obtained in reactivity tests of samples calcined under five different conditions are shown in Figure 8. It can be observed that samples calcined at temperatures up to 800 °C are more reactive, but as the number of cycles increases, the reactivity of all the samples seems to converge to similar values. The results suggest that reactivity of the oxide, as reflected in the CO_2 capture capacities, depends more strongly on the number of cycles than on calcination conditions within the range tested.
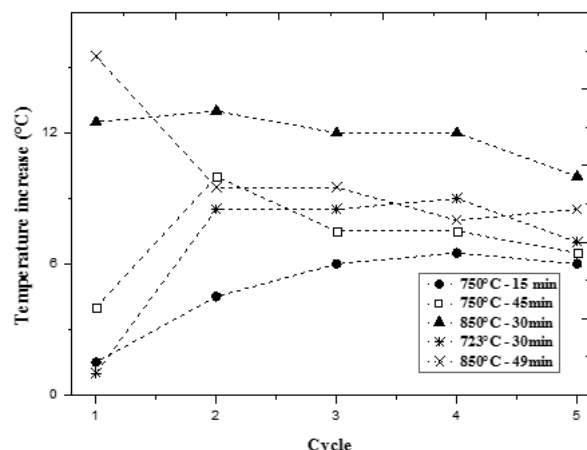
Figure 8: Sorbent reactivity vs. the number of cycles for different calcination conditions.

CONCLUSIONS

In this paper, we have experimentally investigated the CO_2 capture capacity of a high limestone content waste via five calcination-hydration-carbonation reaction cycles under different calcination conditions. The parametric optimization shows that the increase of the calcination temperature and time increases the quality of quicklime and CO_2 capacity capture for the initial cycles, until the best region of operation is reached and then it decreases. Furthermore, for the first cycle, those samples treated at higher calcination temperatures showed better ability to capture CO_2. However, over several cycles, the ability to capture CO_2 for all conditions tended to similar values and the difference between the best and the worst condition tested decreased. Therefore, it appears that the calcination temperature and time influence CO_2 uptake in the initial cycles, but as the number of cycles increases, the effect becomes less significant. The loss of CO_2 capture capacity can probably be attributed to the sintering, which is faster for sorbents calcined at higher temperatures. Although there is a loss in the CO_2 capture capacity of CaO over the cycles for all

samples, which is common for this kind of material, the waste seems to be suitable for CO_2 capture.

REFERENCES

Abanades, J. C. and Alvarez, D., Conversion limits in the reaction of CO_2 with lime. Energy & Fuels, 17, 308 (2003).

Abanades, J. C., Rubin, E. S. and Anthony, E. J., Sorbent cost and performance in CO_2 capture systems. Ind. Eng. Chem. Res., 43(13), 3462 (2004).

Al-Jeboori, M. J., Fennell, P. S., Nguyen, M. and Feng, K., Effects of different dopants and doping procedures on the reactivity of CaO-based sorbents for CO_2 capture. Energy & Fuels, 26, 6584 (2012).

Ar, I. and Dogu, G., Calcination kinetics of high purity limestones. Chemical Engineering Journal, 83, 131 (2001).

Barker, R., The reversibility of the reaction $CaCO_{3(s)} \rightleftarrows CaO_{(s)} + CO_{2(g)}$. J. Chem. Technol. Bioechnol., 23, 733 (1973).

Blamey, J., Anthony, E. J., Wang, J. and Fennell, P. S., The calcium looping cycle for large-scale CO_2 capture. Progress in Energy and Combustion Science, 36, 269 (2010).

Blamey, J., Paterson, N., Dugwell, D., Fennell, P., Mechanism of particle breakage during reactivation of CaO-based sorbents for CO_2 capture. Energy Fuels, 24, 4605 (2010).

Borgwardt, R. H., Calcium oxide sintering in atmospheres containing water and carbon dioxide. Ind. Eng. Chem. Res., 28, 493 (1989).

Garcia-Labiano, F., Abad, A., Diego, L. F., Adanez, J., Calcination of calcium-based sorbents at pressure in a broad range of CO_2 concentrations. Chemical Engineering Science, 57, 2381 (2002).

González, B., Grasa, G. S., Alonso, M. and Abanades, J. C., Modeling of the deactivation of CaO in a carbonate loop at high temperatures of calcination. Ind. Eng. Chem. Res., 47, 9256 (2008).

Grasa, G. S. and Abanades, J. C., CO_2 capture capacity of CaO in long series of carbonation/calcination cycles. Ind. Eng. Chem. Res., 45, 8846 (2006).

Kikkinides, E. S. and Yang, R. T., Concentration and recovery of CO_2 from flue gas by pressure

swing adsorption. Ind. Eng. Chem. Res., 32, 2714 (1993).

Kuramoto, K., Fujimoto, S., Morita, A., Shibano, S., Suzuki, Y., Hatano, H., Shi-Ying, L., Harada, M., Takarada, T., Repetitive carbonation-calcination reactions of Ca-based sorbents for efficient CO_2 sorption at elevated temperatures and pressures. Ind. Eng. Chem. Res., 42, 975 (2003).

López-Periago, A. M., Fraile, J., López-Aranguren P., Vega, L. F. and Domingo, C., CO_2 capture efficiency and carbonation/calcination kinetics of micro and nanosized particles of supercritically precipitated calcium carbonate. Chemical Engineering Journal, 226, 357 (2013).

Manovic, V., Charland, J. P., Blamey, J., Fennell, P. S., Lu, D. Y. and Anthony, E. J., Influence of calcination conditions on carrying capacity of CaO-based sorbent in CO_2 looping cycles. Fuel, 88, 1893 (2009).

Nikulshina, V., Gálvez, M. E., Steinfeld, A., Kinetic analysis of the carbonation reactions for the capture of CO_2 from air via the $Ca(OH)_2$–$CaCO_3$–CaO solar thermochemical cycle. Chemical Engineering Journal, 129, 75 (2007).

Phalak, N., Deshpande, N. and Fan, L. S., Investigation of high-temperature steam hydration of naturally derived calcium oxide for improved carbon dioxide capture capacity over multiple cycles. Energy & Fuels, 26, 3903 (2012).

Ramkumar, S., Fan, L. -S., and Lowrie, W. G., Thermodynamic and Experimental Analyses of the Three-Stage Calcium Looping Process. Ind. Eng.

Chem. Res., 5, No 16, 7563 (2010).

Ridha, F. N., Manovic, V., Macchi, A. and Anthony, E. J., High-temperature CO_2 capture cycles for CaO-based pellets with Kaolin-based binders. Greenhouse Gas Control, 6, 164 (2012).

Santos, E. T., Alfonsín, C., Chambel, A. J. S., Fernandes, A., Dias, A. P. S., Pinheiro, C. I. C. and Ribeiro, M. F., Investigation of a stable synthetic sol–gel CaO sorbent for CO_2 capture. Fuel, 94, 624, (2012).

Sun, P., Grace, J. R., Lim, C. J., Anthony, E. J., Determination of intrinsic rate constants of the CaO–CO_2 reaction. Chemical Engineering Science, 63, 47 (2008).

Symonds, R. T., Lu, D. Y., Macchi, A., Hughes, R. W. and Anthony, E. J., CO_2 capture from syngas via cyclic carbonation/calcination for a naturally occurring limestone: Modelling and bench-scale testing. Chemical Engineering Science, 64, 3536 (2009).

Valverde, J. M., Sanchez-Jimenez, P. E., Perejon, A. Perez-Maqueda, L. A., Role of looping-calcination conditions on self-reactivation of thermally pretreated CO_2 sorbents based on CaO. Energy & Fuels, 27, 3373 (2013).

Yu, F., Phalak, N., Sun, Z. and Fan, L.-S., Activation strategies for calcium-based sorbents for CO_2 capture: A perspective. Ind. Eng. Chem. Res., 51, 2133 (2012).

Zeman, F., Energy and material balance of CO_2 capture from ambient air. Environ. Sci. Technol., 41, 7558 (2007).